A Proposal of a New Dielectric Resonator Construction for MIC's

YOSHIO SHIMODA, HISASHI TOMIMURO, AND KOTA ONUKI

Abstract—**A compact and high-temperature-stable dielectric resonator having no shielding metal walls nor a conventional frequency tuning screw is described. This resonator consists of a high ϵ_r dielectric resonator element mounted on a low-loss dielectric mount, a dielectric disk with thin metal film fixed on the resonator element, and a microstrip line substrate on which to mount the constituents. The resonant frequency tuning is made by trimming the metal film on the disk. The $TE_{01\delta}$-mode resonant frequencies are analyzed through dielectric waveguide model application. Less than 1-percent analytical error is presented in comparison with the experimental data for a practical resonator. The frequency tuning limit by metal film trimming is about 7 percent. The unloaded Q value of 2700 at 8.8 GHz and a 4.4-ppm/deg frequency temperature coefficient are obtained.**

I. Introduction

MANY APPLICATIONS for dielectric resonators have been stimulated due mainly to the recent development of low-loss, temperature-stable dielectric materials [1]–[4]. Temperature-compensated oscillators are one of the applications for microwave integrated circuits (MIC's) [2], [5]. The oscillating frequency of these oscillators is stabilized with a dielectric resonator coupled to a transmission line.

In conventional dielectric resonator configurations for practical MIC applications, a cylindrical dielectric resonator element made of high dielectric constant material is placed on a stripline substrate and shielded with conducting metal walls to suppress radiation. Additionally, a metal tuning screw, attached to one side of the metal walls, is positioned above the dielectric resonator element [2], [5]. The resonant frequencies for conventional resonators have been tuned by adjusting the air gap between the resonator element and the tuning screw. In this tuning system, however, ambient temperature variation may cause undesirable air gap changes and deteriorate the resonant frequency stability, if the thermal expansion design has been made without giving adequate consideration to the metals used in the shielding wall and the tuning screw. Generally, conventional dielectric resonators with shielding walls and a frequency tuning screw have disadvantages in size, in temperature-stability resultant from design, and in manufacturing because of their complicated structures.

This paper describes a new type of dielectric resonator, which does not use shielding walls and a tuning screw. It also presents a new resonant frequency tuning method for this resonator.

Manuscript received August 6, 1982; revised March 8, 1983.

The authors are with Musashino Electrical Communication Laboratory, Nippon Telegraph and Telephone Public Corporation, 3-9-11, Midoricho, Musashino-shi, Tokyo, 180, Japan

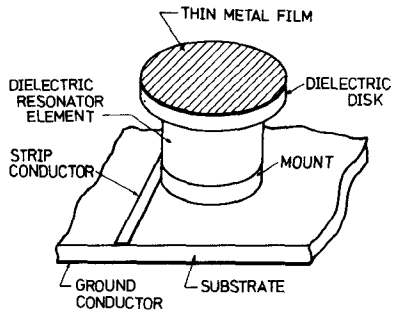

Fig. 1. New dielectric resonator.

Several reports have been made on methods for predicting the resonant frequencies of cylindrical dielectric resonators excited in the $TE_{01\delta}$ mode [6]–[11]. Some of them are very complicated, although they show good accuracy [8], [10], [12]. In this paper, resonant frequencies for the new resonator are analyzed in application of the dielectric waveguide model [9]. The numerical results have sufficient accuracy to allow for the designing of an actual resonator.

II. New Dielectric Resonator

A. Configuration

A new dielectric resonator magnetically coupled to a microstrip line is shown in Fig. 1. The resonator is constructed from a cylindrical dielectric resonator element, a thin metal film attached to a dielectric disk, a mount, and a stripline substrate. The disk and mount are made of low-dielectric constant material. The dielectric resonator element is supported by the mount applied on the stripline substrate. The disk plays the role of a support for the thin metal film which can suppress the electromagnetic radiation from the dielectric resonator element. The thin metal film is fabricated by vacuum deposition of gold over nichrome, followed by gold electroplating. The disk, mount, and substrate materials are required to have relative dielectric constants which are as small as possible in comparison with the resonator element dielectric constant, in order to reduce radiation loss and obtain a high-Q dielectric resonator system. The disk with the thin metal film, the resonator element, and the mount are fixed on the stripline substrate with adhesive as shown in Fig. 1. Table I shows the

0018-9480/83/0700-0527$01.00 ©1983 IEEE

TABLE I
RESONATOR CONSTITUENT MATERIALS AND THEIR PROPERTIES

Constituents	Dielectric resonator element	Disk and mount	Substrate
Materials	BaO-TiO_3 system ceramic	Fused quartz	Alumina ceramic
Relative dielectric constants	39.5	3.8	9.6
Thermal expansion coefficients (ppm/deg)	8.8[a]	0.4[b]	8.1[d]
Dielectric constant temperature coefficients (ppm/deg)	-23.8[a]	-100[c]	200[e]

(a) Data is from reference (2)
(b) Quartz optical and industrial grade selection chart, Nippon Silica Glass Company
(c) Technical data sheet, Corning Glass Works
(d) Technical data sheet, NGK Spark Plug Co. Ltd
(e) Technical data sheet, American Lava Corporation

resonator constituent materials, their relative dielectric constants, and their thermal properties.

This resonator is simple because it does not have shielding walls and a frequency tuning screw used in conventional units. As a result, the resonator size can be compact, and frequency drift caused by metal thermal expansion does not need to be considered.

B. Resonant Frequency Tuning Method

The resonant frequencies of this resonator depend on the distance between the thin metal film and the dielectric resonator element; that is, they depend on the disk thickness. This fact can be conjectured easily from the resonant frequency tuning methods used in conventional resonators. A frequency tuning method by adjusting disk thickness, however, is not practical because the mounting of resonator constituents on the substrate must be carried out simultaneously due to requirements for precise positioning. Consequently, the disk thickness should be determined as a certain value before reaching the component mounting stage.

In this resonator, resonant frequencies are tuned by trimming the thin metal film on the disk. The use of a laser trimmer is helpful for trimming this area. The frequency tuning values obtained analytically and experimentally will be discussed later.

III. RESONANT FREQUENCY ANALYSIS

An analytical model is shown in Fig. 2 for the resonant frequencies of this resonator. The resonators shown in Fig. 2(a) and (b) are called a resonator with a metal film and a resonator with no metal film in this paper. The resonator with a metal film shows the no trimming condition for the metal film. The resonator with no metal film shows the condition after all excess metal was removed by trimming. The resonant frequency tuning limit is obtained from the frequency difference between the resonator with a metal film and the resonator with no metal film.

Basic assumptions in this analysis are as follows.

a) All dielectric materials are isotropic and have no dissipation.

b) Metallic boundaries are perfectly conducting.

c) Electromagnetic field distribution is that of the dominant $TE_{01\delta}$ mode. (Subscripts refer to cylindrical coordinates θ, r, and z, respectively.)

d) The relative dielectric constant of the resonator element is considerably higher than those of other constructions.

e) The thickness of adhesive layers is negligible.

f) The field in regions 6–8 shown in Fig. 2 are ignored.

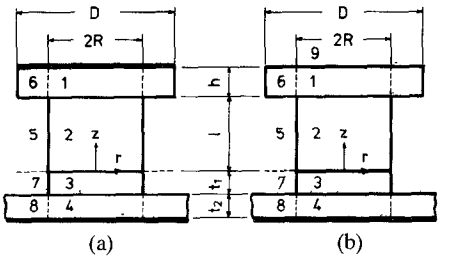

Fig. 2. Cross sections of resonator under analysis and coordinate system. (a) A resonator with a metal film. (b) A resonator with no metal film.

A. Resonant Frequencies for the Resonator with a Metal Film

The resonator to be analyzed can be divided into eight regions, 1–8, as shown in Fig. 2(a). It is assumed that most of the electromagnetic energy is stored in region 2, and that the field decays in regions 1 and 3–5. The field in regions 6–8 is ignored because the energy in these regions is considered to be too small. If the field in region 5 is ignored, it becomes equivalent to the magnetic wall model.

Scalar functions $\Psi_i (i = 1\text{–}5)$ satisfying the Helmholtz equation in each region may be written as follows, considering the boundary conditions at $z = l + h$ and $z = -(t_1 + t_2)$:

$$\Psi_1 = A_1 J_0(k_r r)\sinh\{-\xi[z-(l+h)]\} \tag{1}$$

$$\Psi_2 = J_0(k_r r)\{A_2\cos(k_z z) + B_2\sin(k_z z)\} \tag{2}$$

$$\Psi_3 = J_0(k_r r)\{A_3\cosh(\gamma z) + B_3\sinh(\gamma z)\} \tag{3}$$

$$\Psi_4 = A_4 J_0(k_r r)\sinh\{\eta[z+(t_1+t_2)]\} \tag{4}$$

$$\Psi_5 = A_5 K_0(p_r r)\{A_2\cos(k_z z) + B_2\sin(k_z z)\} \tag{5}$$

where

$$K_r^2 = \epsilon_1 k_0^2 + \xi^2 = \epsilon_2 k_0^2 - k_z^2 = \epsilon_3 k_0^2 + \gamma^2 = \epsilon_4 k_0^2 + \eta^2 \tag{6}$$

$$p_r^2 = k_z^2 - k_0^2 \tag{7}$$

$$k_0^2 = \omega^2 \epsilon_0 \mu_0 = (2\pi f)^2 \epsilon_0 \mu_0 \tag{8}$$

where

2_1–A_5, B_2, B_3	unknown constants,
$J_0(x)$, $K_0(x)$	the Bessel and the modified Hankel functions of order zero,
k_r, p_r	wavenumbers with respect to r,
k_z, ξ, γ, η	wavenumbers with respect to z,
$\epsilon_i (i = 1\text{–}4)$	relative dielectric constants in region i,
ϵ_0, μ_0	dielectric constant and permeability in free space,
ω, f	angular frequency and frequency.

The field components in each region are given by sub-

stituting Ψ_i into the following equations:

$$\left.\begin{aligned} E_{\theta i} &= -j\omega\mu_0 \frac{\partial \Psi_i}{\partial r} \\ H_{ri} &= \frac{\partial^2 \Psi_i}{\partial r \partial z} \\ H_{zi} &= k_r^2 \Psi_i \\ E_{ri} &= E_{zi} = H_{\theta i} = 0 \end{aligned}\right\} \tag{9}$$

where E_θ, H_r, and H_z denote the circumferential component of the electric field, radial, and axial components of the magnetic field, respectively. The field decays in the regions of $r > R$, $z > l$, and $z < 0$.

From the continuity conditions on the field components, the following boundary conditions are introduced:

a) $H_{z2} = H_{z5}$ at $r = R$, for $0 < z < l$

b) $E_{\theta 2} = E_{\theta 5}$ at $r = R$, for $0 < z < l$

and

c) $H_{r1} = H_{r2}$, $E_{\theta 1} = E_{\theta 2}$ at $z = l$, for $0 < r < R$

d) $H_{r2} = H_{r3}$, $E_{\theta 2} = E_{\theta 3}$ at $z = 0$, for $0 < r < R$

e) $H_{r3} = H_{r4}$, $E_{\theta 3} = E_{\theta 4}$ at $z = -t_l$, for $0 < r < R$.

Boundary conditions a) and b) yield the following eigenvalue equation:

$$\frac{J_0'(k_r R)}{k_r J_0(k_r R)} + \frac{K_0'(p_r R)}{p_r K_0(p_r R)} = 0 \tag{10}$$

where $J_0'(x)$ and $K_0'(x)$ represent derivatives with respect to the argument for $J_0(x)$, $K_0(x)$.

Boundary conditions c), d), and e) yield the following eigenvalue equation:

$$\begin{vmatrix} -\xi\cosh A & k_z \sin B & -k_z \cos B & 0 & 0 & 0 \\ 0 & 0 & -k_z & 0 & \gamma & 0 \\ 0 & 0 & 0 & -\gamma \sinh C & \gamma \cosh C & -\eta \cosh D \\ -\sinh A & \cos B & \sin B & 0 & 0 & 0 \\ 0 & 1 & 0 & -1 & 0 & 0 \\ 0 & 0 & 0 & \cosh C & -\sinh C & -\sinh D \end{vmatrix} = 0 \tag{11}$$

where $A = \xi h$, $B = k_z l$, $C = \gamma t_1$, $D = \eta t_2$, and

$$\xi = \left(k_r^2 - \epsilon_1 k_0^2\right)^{1/2} \qquad \eta = \left(k_r^2 - \epsilon_4 k_0^2\right)^{1/2}$$
$$k_z = \left(\epsilon_2 k_0^2 - k_r^2\right)^{1/2} \qquad k_0^2 = \omega^2 \epsilon_0 \mu_0.$$
$$\gamma = \left(k_r^2 - \epsilon_3 k_0^2\right)^{1/2}$$

Resonant frequencies of the resonator with a metal film are determined by solving the pair of eigenvalue equations (10) and (11).

B. Resonant Frequencies for the Resonator with no Metal Film

The resonator with no metal film to be analyzed has to take into account, region 9, in which electromagnetic energy may exist due to there being no metal boundary at $z = l + h$. Therefore, scalar functions in regions 1 and 9 may be assumed to be as follows:

$$\Psi_1 = J_0(k_r r)\{A_1 \cosh[\xi(z-l)] - B_1 \sinh[\xi(z-l)]\} \tag{12}$$

$$\Psi_9 = A_9 J_0(k_r r) \exp\{-\zeta[z-(l+h)]\} \tag{13}$$

where

$$k_r^2 = \epsilon_1 k_0^2 + \xi^2 = k_0^2 + \zeta^2. \tag{14}$$

The scalar functions in the other regions, 2–5, can be considered the same as for expressions (2)–(5). The field components in each region are obtained after substituting these functions into (9).

Applications of continuity conditions on the field components at $r = R$ and $z = -t_1$, 0, l, and $l + h$ lead to the pair of eigenvalue equations shown below. Subsequently, the resonant frequencies for the resonator with no metal film are determined.

$$\frac{J_0'(k_r R)}{k_r J_0(k_r R)} + \frac{K_0'(p_r R)}{p_r K_0(p_r R)} = 0 \tag{15}$$

$$\begin{vmatrix} -\xi & -\xi\sinh A & \xi\cosh A & 0 & 0 & 0 & 0 & 0 \\ 0 & 0 & -\xi & k_z \sin B & -k_z \cos B & 0 & 0 & 0 \\ 0 & 0 & 0 & 0 & -k_z & 0 & \gamma & 0 \\ 0 & 0 & 0 & 0 & 0 & -\gamma \sinh C & \gamma \cosh C & -\eta \cosh D \\ 1 & -\cosh A & \sinh A & 0 & 0 & 0 & 0 & 0 \\ 0 & 1 & 0 & -\cos B & -\sin B & 0 & 0 & 0 \\ 0 & 0 & 0 & 1 & 0 & -1 & 0 & 0 \\ 0 & 0 & 0 & 0 & 0 & \cosh C & -\sinh C & -\sinh D \end{vmatrix} = 0 \tag{16}$$

where $A = \xi h$, $B = k_z l$, $C = \gamma t_1$, and $D = \eta t_2$.

IV. Theoretical and Experimental Resonant Frequencies

Theoretical resonant frequencies are compared with the experimental frequencies in the 8–9-GHz region.

Sample dimensions are as follows. The resonator element

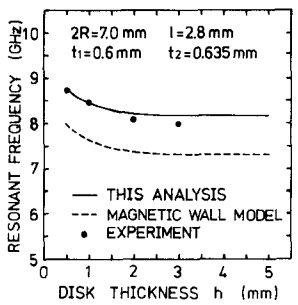

Fig. 3. Resonant frequency versus disk thickness.

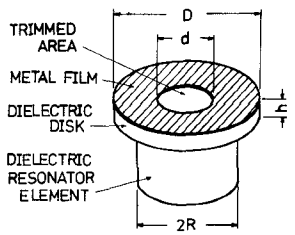

Fig. 4. Metal film trimming.

is 7 mm in diameter and 2.8 mm thick, and the mount and substrate thicknesses are 0.6 mm and 0.635 mm, respectively. The accuracy of these dimensions is within ± 10 μm. The adhesive thickness of about 5 μm is ignored in this resonant frequency analysis.

A. Resonant Frequencies for the Resonator with a Metal Film

Fig. 3 shows the resonant frequency versus disk thickness. The resonant frequencies predicted by the present analysis agree well with the experimental values. When thicknesses are 1 mm, 2 mm, and 3 mm, analytical errors are about 0.3, 1.6, and 2.5 percent, respectively. The use of thick disks leads to poor approximation in this analysis because the amount of electromagnetic energy in region 6 increases.

The resonant frequencies derived by the magnetic wall model are lower than the experimental values by about 8–10 percent. The analytical error is too large to allow for the designing of an actual resonator.

B. Resonant Frequencies for the Resonator with no Metal Film and Frequency Change by Tuning

Computed resonant frequencies for the resonator with no metal film show little dependence on disk thickness. Frequencies are about 8.15 GHz in the 0.5–5-mm disk thickness. The frequency values almost equal those for the resonator with a metal film, in which disk thickness is more than 4 mm.

Resonant frequencies for this compact resonator are tuned by trimming the thin metal film on the disk, as shown in Fig. 4. In order to obtain accurate experimental data, the metal film was trimmed by using photolithography technique. Fig. 5 shows the resonant frequency changes with the metal trimmed area normalized as $d/2R$. Frequency changes caused by trimming increase with decreasing disk thickness. According to the advantages for frequency compensations, the use of thin disks is better for practical resonators.

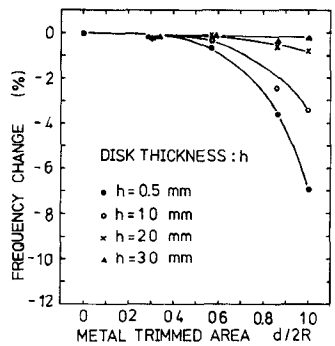

Fig. 5. Frequency change by trimming.

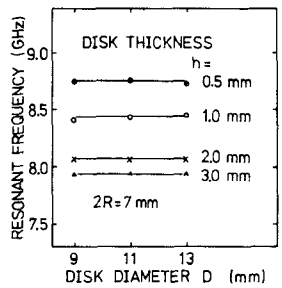

Fig. 6. Resonant frequency versus disk thickness.

C. Resonant Frequencies with Disk Diameters

Resonant frequency dependence, with respect to disk diameter equated to metal film diameter, is shown in Fig. 6 for the resonator with a metal film. Frequencies are independent of disk diameters. The results show that resonant frequencies are unaffected by energy decaying toward the radial direction in region 6 of Fig. 2.

V. Experimental Results of Other Characteristics

A. Unloaded Q

The unloaded $Q(Q_0)$ for the resonator is generally expressed as follows:

$$\frac{1}{Q_0} = \frac{1}{Q_r} + \frac{1}{Q_d} + \frac{1}{Q_c} \tag{17}$$

where Q_r, Q_d, and Q_c are Q-factors due to radiation loss, dielectric loss, and conduction loss, respectively. The radiation loss is related to the resonator structure. The dielectric loss is related to energy loss in the dielectric resonator element, disk, mount, and substrate. The conduction loss is the energy loss in the metal film, and is related to the surface resistivity of the film. For this resonator, most of the electromagnetic energy is stored in the dielectric resonator element and the energy decays in other regions. Therefore, the effects of the dielectric loss other than the dielectric resonator element and the conduction loss for the metal film are considered to be small, so long as their loss values are not significantly large. The loss tangent corre-

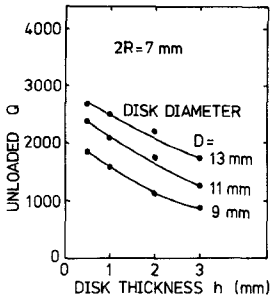

Fig. 7. Resonator unloaded Q versus disk thickness.

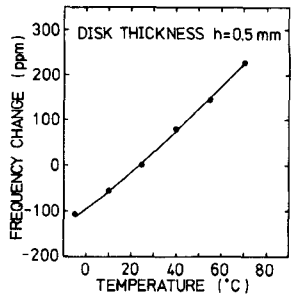

Fig. 8. Frequency temperature dependence for resonator.

sponding to $1/Q_d$ for alumina making up the substrate and for the fused quartz making up the disk and mount are the order of 1×10^{-4}–2×10^{-4} at 10 GHz in contrast to 2.86×10^{-4} for the dielectric resonator element. The conduction loss for the metal film is the order of 1×10^{-4} from an estimation for a conventional cylindrical cavity. Therefore, it is considered that this resonator's unloaded Q is determined by the radiation loss and the dielectric loss of the dielectric resonator element.

Fig. 7 shows the experimental unloaded Q for the resonator with a metal film. The unloaded Q becomes higher as the disk becomes thinner or the diameter larger. The maximum unloaded Q is about 2700 at 8.8 GHz, in contrast to Q_d of 3500 for the resonator element material. Degradation of Q_0 may be attributable to the radiation loss. Use of thin and large diameter disks leads to radiation loss suppression.

The unloaded Q is insensitive to the trimming area of the metal film as long as the area $d/2R$ is 0–0.65 for any disk thickness, and the Q_0 values are about 0.90–0.95 times those for the no-trimming condition. When the trimmed area is large, the trimming effect for the unloaded-Q decrease becomes sensitive for thin-disk resonators due to increase of radiation loss. For example, when the disk thickness is 0.5 mm and the trimmed area $d/2R$ is 0.86, the unloaded Q decreases to 0.7 times the Q_0 value for the no-trimming condition.

Unloaded Q for this resonator can be improved by using low-loss tangent materials for the dielectric resonator element. In one example, the unloaded Q for the resonator with a metal film shows 3400 at 10 GHz when a dielectric resonator element having 9500 inverse loss-tangent and 37.0 relative dielectric constant is used. This unloaded-Q value is comparable to that of conventional type resonator [13].

B. Temperature Dependence of Resonant Frequency

Resonant frequency change with temperature is almost linear in a practical temperature range as shown in Fig. 8. Its temperature coefficient is about 4.4 ppm/deg. The temperature coefficient depends on dielectric constant temperature coefficients and thermal expansion coefficients for the resonator constituents shown in Table I. Temperature effects on the resonant frequency can be computed by substituting these coefficients into the analytical model mentioned in Section III. The value estimated is 3.82 ppm/deg, which approximately agrees with the experimental value. The resonant frequency change caused by the variations of the constants of the dielectric resonator element only is about 3.82 ppm/deg. On the other hand, the effect of the disk, mount, and substrate is less than 0.01 ppm/deg, which is negligible as compared with the value for the dielectric resonator element. Therefore, the resonant frequency temperature dependence for this resonator structure is mainly determined by the constants of the dielectric resonator element.

The resonant frequency temperature coefficient η_f is generally approximated as follows [2]:

$$\eta_f \simeq -\frac{1}{2}\eta_\epsilon - \alpha \tag{18}$$

where η_ϵ is the dielectric constant temperature coefficient and α is the thermal expansion coefficient.

By substituting the numerical values for the dielectric resonator element shown in Table I, the η_f value becomes 3.1 ppm/deg. This value is somewhat small when compared with the experimental value 4.4 ppm/deg and the value 3.82 ppm/deg computed by this analytical model. The temperature coefficient estimated by our model is more reasonable for this resonator structure. When the disk thickness is more than or equal to 2 mm, the η_f values estimated by our model for the dielectric resonator element approach the value obtained from (18), that is, 3.1 ppm/deg. However, the temperature coefficient for this resonator system including all constituents is almost constant and its value is approximately 3.8 ppm/deg.

VI. Conclusion

A new type of dielectric resonator which consists of a dielectric resonator element, a mount, and a thin metal film attached to a dielectric disk was developed. Because of its configuration calling for no shielding walls and no frequency tuning screw, compact and high-temperature-stability resonators are expected. Their simple configuration will lead to a simple manufacturing process.

Resonant frequency tuning is done by metal film trimming on the dielectric disk.

Resonant frequencies have been analyzed in the application of the dielectric waveguide model. The differences between analytical and experimental resonant frequency are in the allowable range for the design of a practical resonator.

Resonant frequency tuning ranges, which are adjustable by metal film trimming, have been presented as functions of the trimmed area and disk thickness.

Typical characteristics for the resonator are about a 7-percent frequency tuning limit, an unloaded-Q value of 2700 maximum at 8.8 GHz, and a frequency temperature coefficient of 4.4 ppm/deg. The unloaded Q is improved by use of low-loss tangent materials for the dielectric resonator element. The frequency temperature coefficient is mainly determined by the characteristics of the dielectric resonator element.

ACKNOWLEDGMENT

The authors wish to thank H. Sato, J. Kato, and H. Jumonji for their support and encouragement during the course of this work. They also thank K. Sawamoto, T. Uno, and K. Kawano for their helpful comments and discussions.

REFERENCES

[1] J. K. Plourde, D. F. Linn, H. M. O. Bryan, Jr., and J. Thomson, Jr., "$Ba_2Ti_9O_{20}$ as a microwave dielectric resonator," *J. Amer. Ceram. Soc.*, vol. 58, pp. 418–420, Oct.–Nov. 1975.

[2] H. Abe *et al.*, "A highly stabilized low-noise GaAs FET integrated oscillator with a dielectric resonator in the *C* band," *IEEE Trans. Microwave Theory Tech.*, vol. MTT-26, pp. 156–162, Mar. 1978.

[3] S. Kawashima *et al.*, "Dielectric properties of $Ba(Zn_{1/3}Nb_{2/3})O_3 - Ba(Zn_{1/3}Ta_{2/3})O_3$ ceramics at microwave frequency," in *Proc. 1st Meet. Ferroelectric Materials and Their Applications*, 1977, pp. 293–296.

[4] J. K. Plourde *et al.*, "A dielectric resonator oscillator with 5 ppm long term stability at 4 GHz," in *IEEE MTT-S Int. Microwave Symp.*, June 1977, pp. 273–276.

[5] J. K. Plourde and Chung-Liren, "Application of dielectric resonators in microwave components," *IEEE Trans. Microwave Theory Tech.*, vol. MTT-29, pp. 754–770, Aug. 1981.

[6] H. Y. Yee, "Natural resonant frequencies of microwave dielectric resonators," *IEEE Trans. Microwave Theory Tech.*, vol. MTT-13, p. 256, Mar. 1965.

[7] S. B. Cohn, "Microwave bandpass filters containing high Q dielectric resonators," *IEEE Trans. Microwave Theory Tech.*, vol. MTT-16, pp. 218–227, Apr. 1968.

[8] Y. Konishi, N. Hoshino, and Y. Utsumi, "Resonant frequency of a $TE_{01\delta}$ dielectric resonator," *IEEE Trans. Microwave Theory Tech.*, vol. MTT-24, pp. 112–114, Feb. 1976.

[9] T. Itoh and R. Rudokas, "New method for computing the resonant frequencies of dielectric resonators," *IEEE Trans. Microwave Theory Tech.*, vol. MTT-25, pp. 52–54, Jan. 1977.

[10] M. Jaworski and M. W. Pospieszalski, "An accurate solution of the cylindrical dielectric resonator problem," *IEEE Trans. Microwave Theory Tech.*, vol. MTT-27, pp. 639–642, July 1979.

[11] R. Bonetti and A. Atia, "Design of cylindrical dielectric resonators in inhomogeneous media," *IEEE Trans. Microwave Theory Tech.*, vol. MTT-29, pp. 323–326, Apr. 1981.

[12] Y. Kobayashi, N. Fukuoka, and S. Yoshida, "Resonant modes for a shielded dielectric rod resonator," *Trans. IECE Japan*, vol. J64-B, no. 5, pp. 433–440, 1981.

[13] M. Iwakuni *et al.*, "13 GHz highly stabilized feedback oscillator," Paper of the Technical Group on Microwave, IECE, Japan, MW81-2, 1981.

Yoshio Shimoda was born in Tokyo, Japan, in 1948. He received the B.S. degree and completed the graduate course in electrical engineering at Kogakuin University, Tokyo, in 1971 and 1972, respectively.

He joined the Electrical Communication Laboratory, Nippon Telegraph and Telephone Public Corporation, in 1967. He has engaged in research on high-voltage capacitors for submarine cable systems and microwave integrated circuits for radio transmission systems. His current researches are directed toward development of acoustic devices and their applications. He is presently an Engineer of the Musashino Electrical Communication Laboratory, N.T.T.

Mr. Shimoda is a member of the Institute of Electronics and Communication Engineers of Japan, and the Japan Society of Applied Physics.

Hisashi Tomimuro was born in Kawasaki, Japan, in 1949. He received the B.S. degree in control engineering from Tokyo Institute of Technology, Tokyo, Japan, in 1972.

He joined Musashino Electrical Communication Laboratory, Nippon Telegraph and Telephone Public Corporation, in 1972, and has been engaged in the research and development of microwave integrated circuits for radio transmission systems. He is now a Staff Engineer of the Musashino Electrical Communication Laboratory, N.T.T.

Mr. Tomimuro is a member of the Institute of Electronics and Communication Engineers of Japan.

Kota Onuki was born in Sendai, Japan, on August 10, 1938. He received the B.S. and M.S. degrees in physics from the Gakushuin University, Tokyo, in 1964 and 1966, respectively.

He joined the Electrical Communication Laboratory, Nippon Telegraph and Telephone Public Corporation, Tokyo, in 1966, and has engaged in research and development of parts for communication systems. He is presently a Staff Engineer of the Musashino Electrical Communication Laboratory.

Mr. Onuki is a member of the Institute of Electronics and Communication Engineers of Japan, the Japan Society of Applied Physics, and the Physical Society of Japan.